Velocity Measurement of Cosmic Muons using the India-based Neutrino Observatory prototype detector

G.Majumder [a], S.Mohammed [b], N.K.Mondal [a], S.Pal [a,*], D.Samuel [a], B.Satyanarayana [a],

[a] *Department of High Energy Physics, Tata Institute of Fundamental Research, Mumbai 400005, India.*
[b] *Department of Physics, Aligarh Muslim University, Aligarh, 202002, India.*

Abstract

The India-based Neutrino Observatory (INO) collaboration is planning to set up a magnetised 50 kton Iron-Calorimeter with Resistive Plate Chambers (RPC) as active detectors to study neutrino oscillations. A prototype detector stack (without magnet) comprising of 12 layers of RPCs of 1m x 1m in area has been set-up to track cosmic ray muons. To study its capability and the feasibility of distinguishing between up-going and down-going particles, the velocity of cosmic muons recorded in this stack has been measured. The measurement procedure, calibration and results are described here.

Key words: INO, cosmic muons, velocity

1. Introduction

A detailed description of the INO project can be found in other articles in this proceeding [1][2]. The prototype detector stack (without the magnet) for this project has been developed at the Tata Institute of Fundamental Research (TIFR). The detector consists of 12 layers of 1m x 1m RPCs with 32 strips on either readout electrodes labeled as X and Y, with the strips in the X plane orthogonal to the strips in the Y plane. The width of the strips is 2.8cm and the gap between adjacent strips is 0.2cm. The layers are stacked on top of each other, separated by a distance of 16cm which amounts to a total stack height of 1.76m. Fig.1 shows the schematic diagram of the prototype stack. The RPCs are operated in the avalanche mode and the efficiency of the layers are about 95% at an operating voltage of 9.9kV. The time resolution of the chambers is ~ 1.5ns. An overview of the detector set-up can be found in [3][4]. A short description of the detector signal processing units and the DAQ can be found in [5] in this proceeding.

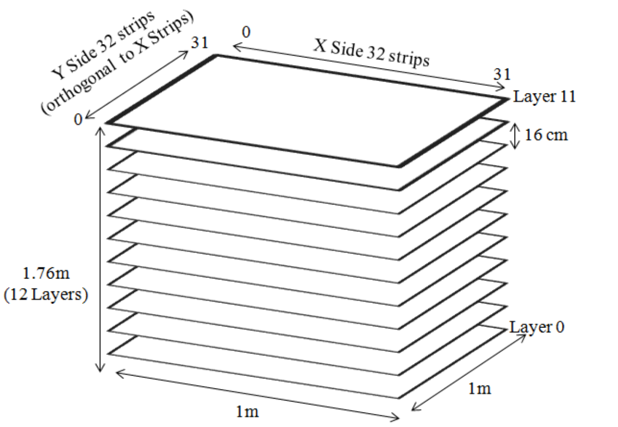

Fig. 1. Schematic diagram of the prototype stack with 12 RPCs.

2. Measurement Procedure

The measurement of the velocity of the particles involves the estimation of the path length traversed by them in the detector and the time taken for the same. The estimation of these parameters is explained in the following sections.

2.1. *Data received from the DAQ*

The following informations are recorded by the DAQ system:

* *Email address:* sumanta@tifr.res.in (S.Pal).
1

– Strip hit information, i.e., the strip-wise hit patterns in the X and Y planes in the layers through which the particle, satisfying the trigger condition (8/12 layer coincidence) has passed through.
– Timing information, measured by a multi-hit TDC (V1190B,CAEN) with 100ps LSB.
– Noise rate of the strips, monitored at regular intervals.

2.2. *Estimation of the path length*

From strip hit information, the slope and the intercept are estimated by fitting a straight line to the respective hit pattern (cf.Fig.2.2).

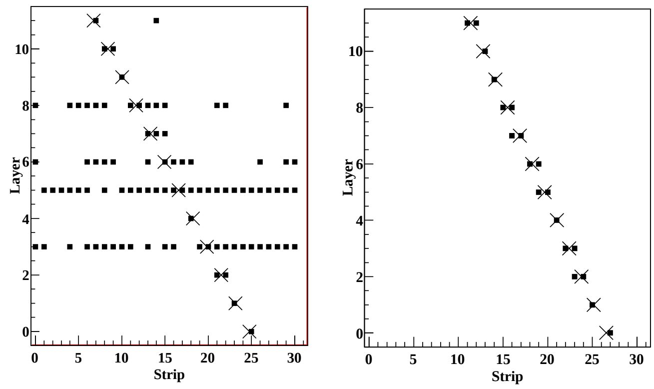

(a) Noisy Event (b) Good Event

Fig. 2. 2(a) shows a typical noisy event and 2(b) shows a proper event. The solid squares are the hits and the crosses are points from the straight line fit made using the algorithm discussed here.

Although the average cluster size is around 1.6 strips, there are however outliers present in the hit pattern arising mainly due to correlated electronic noise. Therefore, data reduction becomes necessary before fitting. X-side and Y-side data are fit separately. The procedure for data reduction and fitting is described below:

(i) First, layers with no hits or with multiplicity greater than 2 are rejected (as in Layers 3,5,6,7,and 8 in Fig.2(a)).
(ii) If the multiplicity is 2, the layer is rejected if the hits are away by 2 strips (as in Layer 11 in Fig.2(a)). Otherwise, the average of the two hits is taken to be the hit position (as in Layers 10 and 2 in Fig.2(a)).
(iii) The event is rejected, if the number of layers is less than 4.
(iv) If the event is accepted, a linear fit is made to the hits.
(v) If the residual (|Fit-Hit|) is greater than 2 strips, the layer is rejected.
(vi) The event is rejected if the number of layers is now less than 4. If accepted, another linear fit is made and the results are saved.

The above procedure results in rejection of approximately 5% of the events. The overall layer rejection is 8%. The error for the hit position is taken as ~ 0.8cm assuming an uniform distribution of the hits along the strip width. This is also getting reflected in the residual distribution. The reduced χ^2 distribution and the residual distribution is shown in Fig.3.

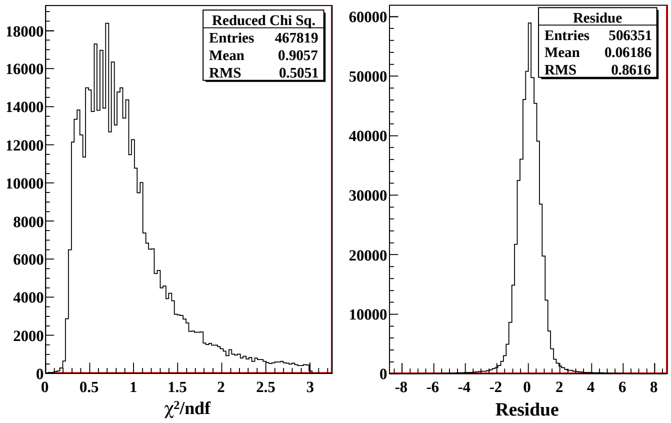

Fig. 3. Reduced χ^2 distribution and the residual distribution for the linear fit to X plane hits.

The total path length l between the plane of the top layer and the plane of the bottom layer is given by:

$$l = \sqrt{(x_2 - x_1)^2 + (y_2 - y_1)^2 + (z_2 - z_1)^2} \quad (1)$$

where (x_1, y_1, z_1) are the coordinates in the plane of the bottom layer and (x_2, y_2, z_2) are the coordinates in the plane of the top layer which are estimated from the linear fit. The zenith angle θ of a track is given by:

$$\theta = \cos^{-1}(\frac{h}{l}) \quad (2)$$

where h is the stack height.

2.3. *Timing Measurement*

Before using the timing data for velocity estimation, a calibration is made so as to correct the differences in propagation delay from strip to strip due to the fact that each strip signal takes its own path to the TDC.

2.4. *Time Offset Calibration*

Since the RPCs operate in the avalanche mode, the signals are amplified by pre-amplifiers with a gain factor of 80. These signals are further processed by Analog Front-Ends (AFE) and Digital Front-Ends(DFE) and finally reach the TDC and other measuring devices in the DAQ. In each plane (X and Y side separately), strips 0-3, 8-11, 16-19 and 24-27 are read by one AFE and strips 4-7, 12-15, 20-23 and 28-31 are read by another AFE. We have assumed that the effective contribution to the time delays come mainly from the electronics succeeding the pre-amplifier stage viz., the AFEs and the DFEs. The schematic for the time offset calibration is shown in Fig.4. For this calibration, the bottom layer (0^{th} Layer) is set as the reference. To calibrate the nth layer, one of the fan-out signal F_n from the pulse generator is connected to its respective AFE (AFE_n). Fan-out F_0 is connected to the AFE of the reference layer and F_t is connected to the trigger input of the TDC. If ΔC is the pulse propagation time from the pulse generator fan-out to AFE and Δt is the pulse propagation time from AFE to the respective TDC channel, then the pulse propagation time difference between the reference layer and the calibrated layer is given by

$$\Delta t = (\Delta C_0 - \Delta C_n) + (\Delta t_0 - \Delta t_n) \qquad (3)$$

To minimize systematic errors, the fan-out channels are swapped at the AFE input and the measurement is repeated. The time difference is now given by

$$\Delta t_{swap} = (\Delta C_n - \Delta C_0) + (\Delta t_0 - \Delta t_n) \qquad (4)$$

The corrected time offset is thus given by

$$\Delta t_{offset} = (\Delta t + \Delta t_{swap})/2 \qquad (5)$$

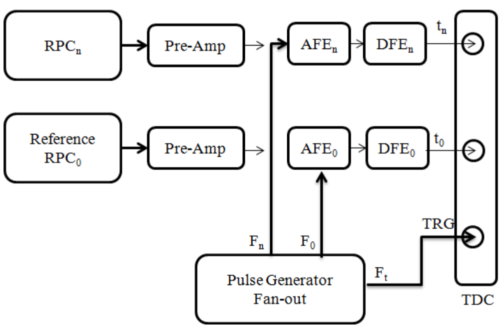

Fig. 4. Schematic of time calibration circuit

The relative time differences for every strip in the different layers were measured and these data were used to correct the timing data. The time offsets with their corresponding error bars for the X and Y planes is shown in Fig.5. The shown plot is the time offsets between the 31^{st} strip of the reference layer and the 31^{st} strip of the corresponding layer. The strip-wise time offsets for 0^{th} layer and 8^{th} layer is shown in Fig. 6.

3. Results

The data presented on this analysis is taken from a run lasting of 24 hours ($\sim 5,00,000$ events). After correcting for the timing offsets, the data (l_i, t_i) is fit to a straight line of the form:

$$t_i - t_0 = \frac{l_i}{v} \qquad (6)$$

where l_i is the track length from 0^{th} layer (bottom layer) to ith layer. t_0 and t_i are the TDC times for 0^{th} layer and ith layer respectively, after applying the corrections. v is the velocity of the particle. Both X and Y timing data are used in the fit. The following procedure was followed for the time-length fit.

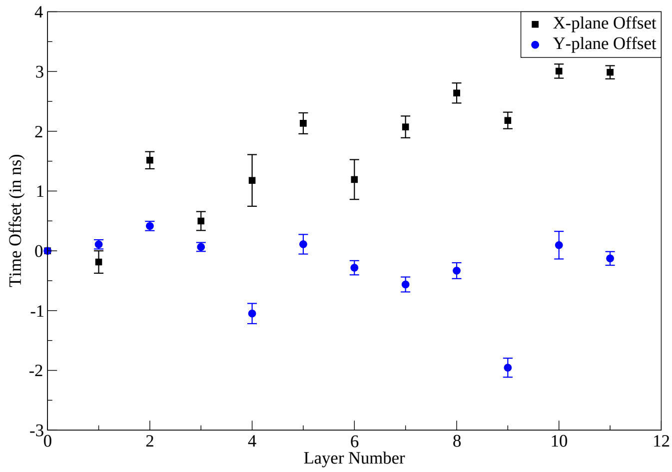

Fig. 5. Layer-wise time offsets for the X and Y planes.

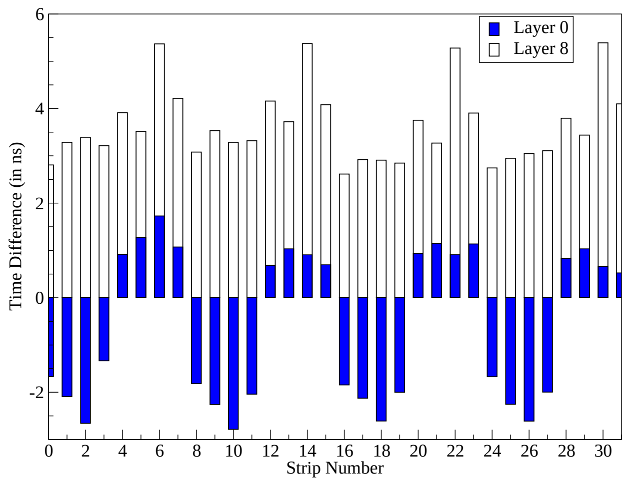

Fig. 6. Strip-wise time offsets for 0^{th} layer and 8^{th} layer. A correlation is seen among strips $i, i+8, i+16$ and $i+24$ due to the fact that they are wired-OR in the AFEs.

- Only tracks that traverse the entire stack are considered. This condition is imposed by an appropriate cut on the zenith angle (0°-38°).
- An event is also rejected if the reference layer (0^{th} layer) timing is not recorded.
- A first linear fit is made if the number of layers is at least 4.
- Points that are more than 2ns away from the straight line are removed.
- The event is rejected if the number of layers is less than 4. Otherwise, a final fitting is made and the results are saved.

The above procedure results in a further rejection of approximately 3-5% of the events. The overall layer rejection is $\sim 8\%$. The velocity distribution is plotted in Fig.7. The reduced χ^2 distribution together with the time residual (|Fit-Hit|) distribution is plotted in Fig.8. The velocity distribution plot in logarithmic scale reveals the presence of a small number of events with negative velocity (0.3% of the total entries). A visual screening of those events in the negative side showed that these events arise from uncorrelated points (cf.Fig.9). Such entries could not be rejected on a generic criterion like a χ^2 cut and there is no clue so far to the origin of such points. The initial timing values (offset corrected) and the final fit are shown in Fig.9. Layer 1 is rejected as no timing is recorded. The 0^{th} layer and the 2^{nd} layer are rejected after the first fit (residue is >2ns). X-timing of 3^{rd} layer and Y-timing of layers 4,6 and 7 are also rejected under the same criteria.

To see the effect of the number of contributing planes to the β distribution, the distribution of β for low number of contributing planes (4-6 layers) and for high number of contributing planes (10-12 layers) were made (Refer. Fig. 7). As seen from the plot, the number of outliers slightly increase for low number of contributing planes.

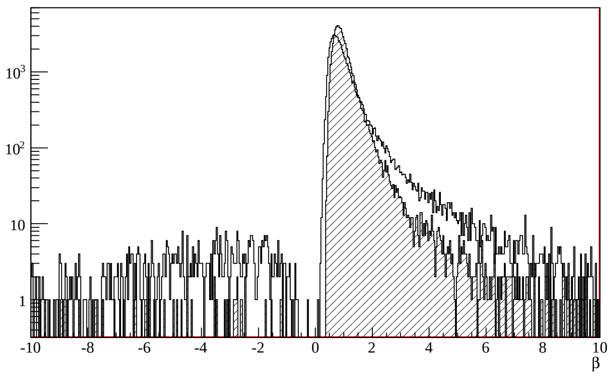

Fig. 7. The β distribution for low number of contributing planes and high number of contributing planes (shaded plot).

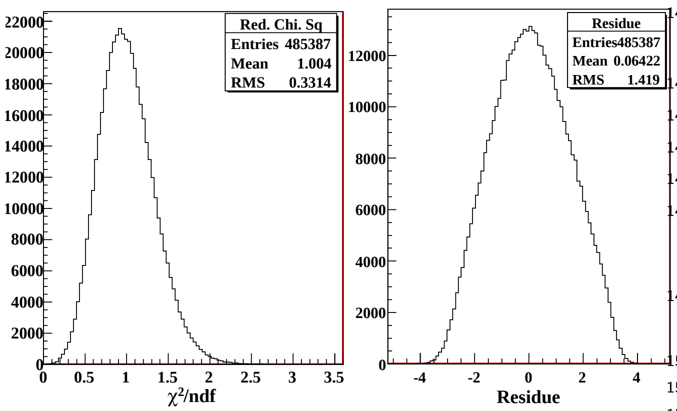

Fig. 8. The reduced χ^2 distribution and the time residual distribution for the linear fit to the timing data.

4. Conclusion

So far the prototype RPC stack has been used to study the detector related parameters. This work is the first step towards a particle physics oriented analysis. The aim of this work is to study the feasibility of using this detector to distinguish between up-going and down-going particles. Since

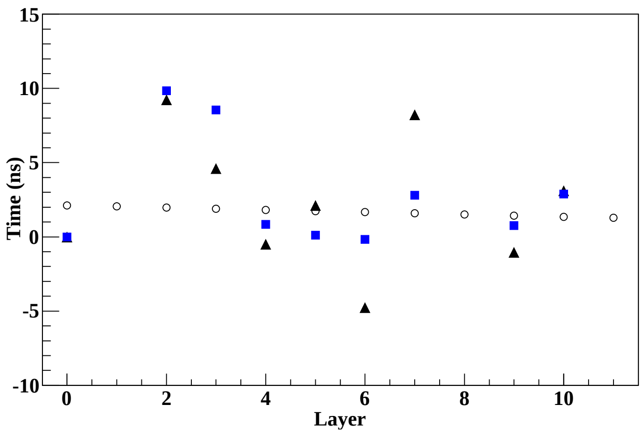

Fig. 9. Timing data of a typical event which results in a negative velocity. The solid squares and the solid triangles represent the X and Y timing respectively. The hollow circle is the second and final straight line fit to these points.

upward-going cosmic muons are stopped by the earth, they can not be observed in the detector. The other source of upward-going muons is from neutrino induced interactions. However, this flux is very small ($\sim (1-4)\times 10^{-15} cm^{-2}s^{-1}$) [6] to be observed in this small detector and in this short period of observation. With the results discussed here, it seems possible to determine the directionality of particles provided the negative part of the β distribution is cleaned up by a well defined rejection criterion. This study has opened up other issues related to timing calibration and analysis that need to be addressed and which might be helpful for the final set-up.

Acknowledgments

The INO project is funded by the Department of Atomic Energy(DAE) and the Department of Science and Technology (DST), Government of India. Crucial contributions from many INO collaborators to this paper are gratefully acknowledged.

References

[1] B.Satyanarayana, et al. Development of 2m x 2m size Glass RPCs for INO, in these proceedings 2010.

[2] N.K.Mondal, et al. Cosmic Ray test of INO RPC stack, in these proceedings 2010.

[3] N.K.Mondal, et al. Development of glass Resistive Plate Chambers for the INO experiment, Nucl. Inst. and Meth. 602A (2009) 744.

[4] B.Satyanarayana, et al. INO prototype detector and data acquisition system, Nucl. Inst. and Meth. 602A (2009) 784.

[5] D.Samuel, et al. VME-based Data Acquisition System for the India-based Neutrino Observatory prototype detector, in these proceedings 2010.

[6] K.Abe, et al. High Energy Neutrino Astronomy using upward-going muons in Super-KamiokandeI, The Astro.Phys.Journal, Vol. 652 (1).